



Thermal behavior of Sicilian clay-based geopolymers

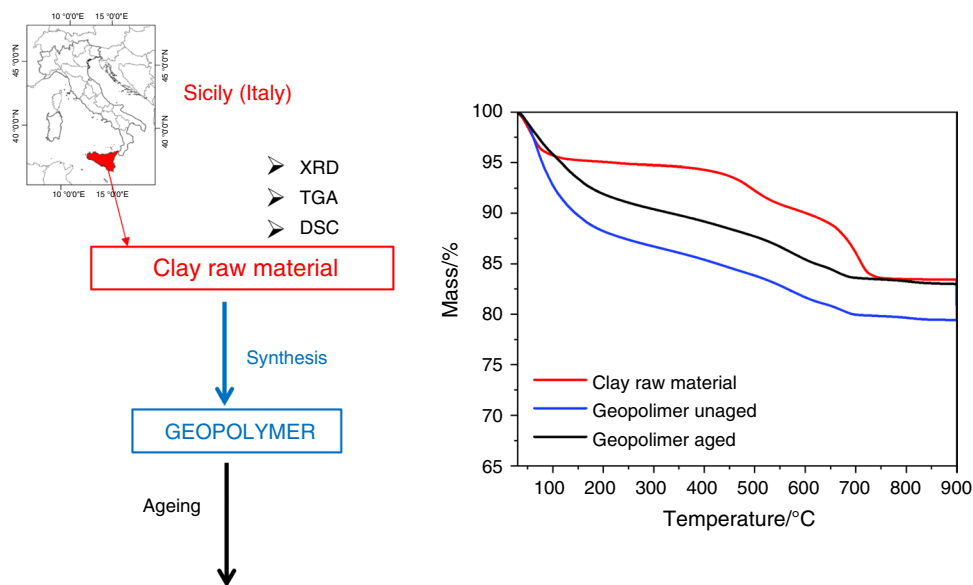
Elena Pulidori¹ · Chiara Pelosi¹ · Maura Fugazzotto² · Silvia Pizzimenti¹ · Maria Rita Carosi¹ · Luca Bernazzani¹ · Antonio Stroschio² · Maria Rosaria Tine¹ · Paolo Mazzoleni² · Germana Barone² · Celia Duce¹

Received: 31 October 2023 / Accepted: 14 April 2024
© The Author(s) 2024

Abstract

Geopolymers have been recently proposed for restoration of built heritage to substitute traditional mortars. Local materials and industrial wastes from the Italian region Sicily showed their potential as low-cost aluminosilicate sources for the preparation of geopolymers. Here, a set of Sicilian clays was studied by Thermogravimetry (TG) and Differential Scanning Calorimetry (DSC), and its mineralogical composition was evaluated by X-ray diffraction (XRD). The raw materials were used to prepare geopolymers by alkaline activation with or without the addition of silicate. The thermal degradation profile of the final materials was studied by TGA and compared with that of the precursors, and the energetics of dehydration were investigated by DSC. Two statistical analyses (made by Principal Component Analysis) were performed on the TG data of raw materials and geopolymers and on the TG data of geopolymers and their mineralogical composition, respectively. The last analysis in particular showed a correlation between the mineralogical composition of the materials and the samples' thermal properties. Additional studies of samples subject to accelerated aging by UV irradiation and exposure to acetic acid vapors highlighted the different effects of these two agents on the samples' stability.

Graphical abstract



Keywords Alkali-activated materials · Thermal degradation · Thermogravimetry · Sicilian clays · Geopolymers

Elena Pulidori and Chiara Pelosi have contributed equally to the work.

Extended author information available on the last page of the article

Introduction

In recent years, the field of construction materials science has been subjected to remarkable transformation driven by the research of sustainable and green alternatives to traditional cement-based materials [1]. Alkali-activated materials (AAMs), formed by polycondensation reactions promoted by an alkaline solution on an aluminosilicate source [2], are promising alternatives widely studied for their good mechanical properties, durability, and significantly reduced carbon emission compared to conventional Portland cement-based materials or traditional ceramics. Among AAMs, geopolymers are the subgroup with the lowest content of calcium [3], but also hybrid systems could be formed [4, 5].

Two main classes of powdered precursors can be used in the alkaline activation process employed to form geopolymers: (1) natural products, such as clay sediments ([6] and reference therein) or volcanic ash [7, 8] and (2) waste industrial materials, such as fly ash from coal combustion power plants [9, 10], blast furnace slags [11], or ceramics wastes [12, 13]. Among the natural raw materials, the most used are sediments mainly formed by clay minerals such as kaolinite, illite, and smectite. To become highly reactive under alkaline conditions, clay sediments need to be calcined, which means thermally activated [6]. The required temperature necessary for their calcination ranges between 500 °C and 800 °C and is therefore considerably lower than those used to create cements and ceramic materials [14, 15]. AAMs have been recently proposed for restoration of built heritage to substitute traditional mortars, as well as in many other kinds of interventions, both esthetical and structural [16–19].

Every built territory in the world is strictly interconnected with the geological resources available in that area, in addition to possible commercial policies that can determine the use of a particular lithotype in a different context with respect to its provenance. Thus, in a land with a huge extension of clay formations as it is the Italian island of Sicily, monuments and historical buildings are frequently realized by products obtained with those clays, such as ceramics, plasters, and mortars. Even if the availability of natural deposits is drastically reduced today, using local clays for restoration in Sicily could be a key strategy to promote a compatible and efficient intervention in the conservation field. Furthermore, the choice to use these materials as precursors for alkali-activated products is driven by their low cost, due especially to the reduction of transport distances, and their easy attainability in the local context, since emerging on the surface of not densely inhabited areas [20, 21]. In this frame, a comparative

characterization among raw materials and AAMs synthesized is an important step to understand if these theoretically highly potential materials are concretely so.

This paper aims to expand the existing data collection by exploring the thermal properties of a novel set of geopolymers made from clay sediments collected in Sicily and belonging to different geological formations. Thermogravimetric analysis (TGA) and Differential Scanning Calorimetry (DSC) were applied to characterize the thermal degradation process (dehydration, dehydroxylation, and decarbonation phenomena) of the geopolymers and the starting raw materials. The effect of different preparation conditions (e.g., metakaolin quantity, NaOH solution concentration, and additive addition) on thermal stability was tested, and the differences among the samples were highlighted by a statistical analysis performed by Principal Component Analysis (PCA). An additional statistical analysis was also permitted to correlate the thermal behavior of the geopolymer samples with their mineralogical composition. Finally, as the final aim of the geopolymers preparation is their use in buildings restoration, their thermal stability after artificial aging conditions was also tested, to assess their resistance to atmospheric agents, e.g., solar radiations or acid vapors.

Materials and methods

Materials

All the clayey sediments selected for this work were sampled in different parts of Sicily (Fig. 1). They present different mineralogical and chemical compositions. The list of the raw materials selected, their abbreviations, and further details are reported in Table 1. The list of geopolymers prepared and analyzed is reported in Table S1.

Geopolymers synthesis

For this work, PP and NU samples were selected, on the basis of their chemical and mineralogical composition, for the AAMs synthesis. As a preliminary treatment, clay materials were firstly dried at 100 °C in an oven for 1 h, milled, and then thermally treated at 700 °C for 3 h to dehydroxylize the clay minerals and make them more reactive to alkaline attack [22–24]. The raw materials were activated either with only sodium hydroxide solutions (NaOH 4M, 6M, and 8M) or with the addition of sodium silicate provided by Ingessil Srl, indicated as R3, having a molar ratio $\text{SiO}_2/\text{Na}_2\text{O} = 3$. In the last case, different NaOH/Na₂SiO₃ ratios were considered in order to investigate the best conditions to avoid efflorescence on samples surface after air exposition. The Liquid/Solid (L/S) ratio is an important factor to consider,

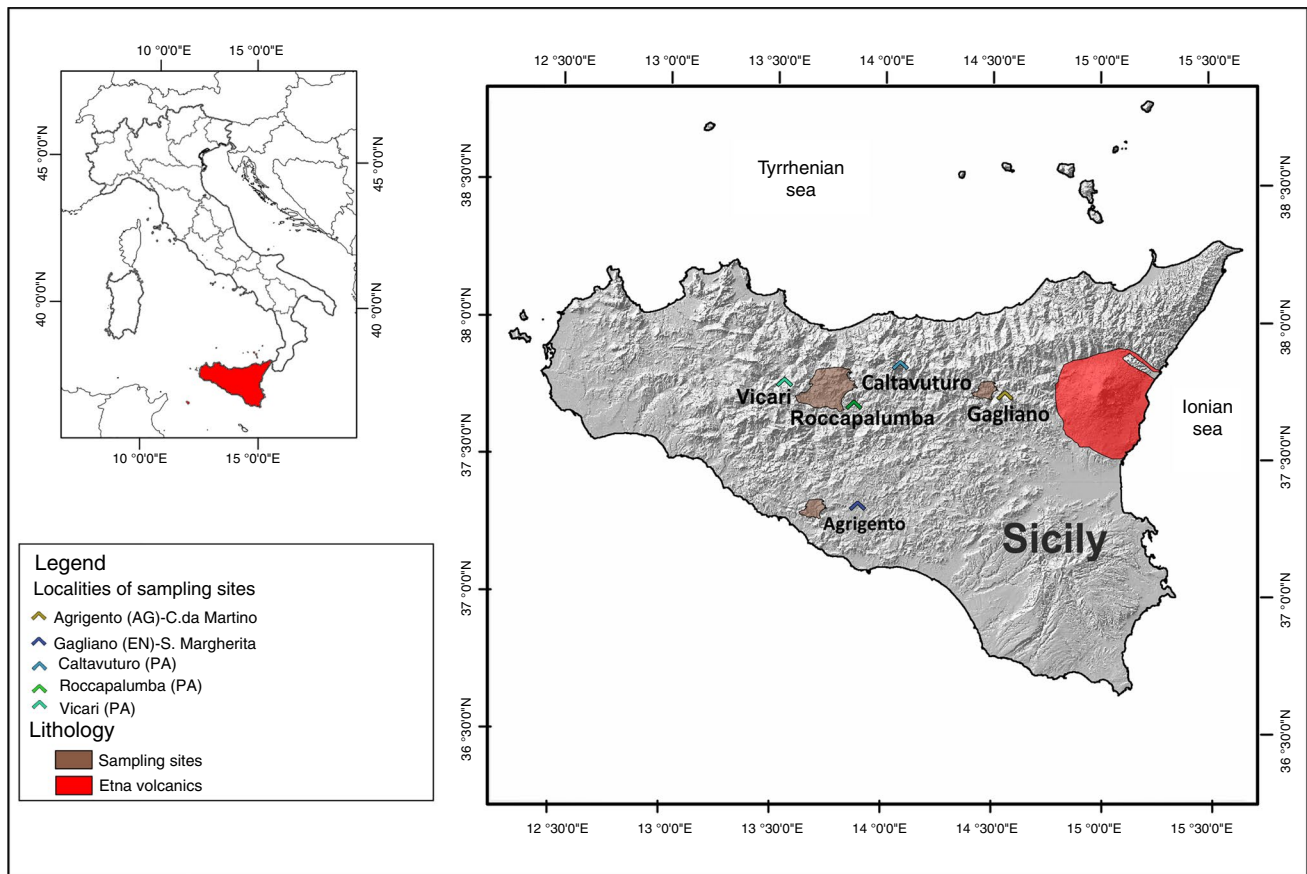


Fig. 1 Sampling sites of the clay raw materials utilized in this paper

Table 1 List of clay sediments selected and sampled

Label ^a	Clay formation	Sampling area
PP	Plio-Pleistocenic clay of Mt. Narbone Formation (Di Grande and Giandinoto, 2022)	C.Da Martino near Agrigento
NU	Numidian clay of Mt. Salici Unit (Barbera et al., 2014)	S.Margherita near Gagliano
RP	Marly clay of Mufara Formation	Roccapalumba
MU	Marly clay of Mufara Formation	Vicari
VC	Variegated clay of the Sicilide Unit	Caltavuturo

^aThe same label with the addition of “700” is referred to the same raw material calcined at 700 °C

during the preparation of the samples, in order to obtain a highly viscous paste and for casting it in the molds. For each formulation, it has been chosen an L/S ratio variable from 0.40 to 0.58. For each formulation, the pastes were mixed for 5 min using a mechanical mixer, and then they were cast in molds of $2 \times 2 \times 2$ cm³ in size. The air bubbles were removed by means of a mechanical vibrator. All samples were cured at room temperature (22 ± 3 °C) for 28 days keeping the humidity level always > 90%. At the end of curing, demolded geopolymers appear intact and without visible cracks. After the curing, only a small quantity of efflorescence was visible in some samples. All the information

regarding the geopolymers formulation and the procedure to synthesize them are reported in [25]. The list of geopolymers prepared and analyzed is reported in Table S1.

Analytical methods

All the raw material samples (untreated and calcined at 700 °C) and the obtained geopolymers underwent X-ray diffraction (XRD) and thermogravimetric measurements (TGA). Selected samples were also analyzed by Differential Scanning Calorimetry (DSC) and subjected to TG analysis after treatment of artificial aging. The overall TGA dataset

(raw materials and geopolymers) was processed by Principal Component multivariate Analysis (PCA). XRD and TGA data of geopolymers alone were processed by additional PC analysis, which aimed to highlight the correlation between their mineralogical composition and thermal behavior.

Powder X-ray diffraction (XRD): XRD was carried out with Rigaku Miniflex II in order to define the mineralogical composition. The instrumental conditions used are: Cu K α radiation; Ni filter; 2 θ angle 5–65°, angular step of 0.01° 2 θ ; step time 5 s; divergence and antiscatter slits of 1°; and receiving slit of 0.2 mm. Clay minerals were analyzed on oriented <2- μ m grain size fraction scanned from 2 θ to 35° 2 θ with a 0.02° 2 θ step size and a 4-s count time at 30 mA and 40 kV. The presence of swelling clay minerals was determined by treating samples with ethylene glycol at 60 °C for 12 h [26]. The semi-quantitative esteem of the clay minerals abundances was obtained by means of the combination profiles of pure-mineral reflection obtained by Newmod software. The best-fit analysis was performed by using the LINEST function in a homemade Excel macro [27].

Thermogravimetric measurements (TGA): Thermogravimetric measurements were taken with a thermobalance from TA Instruments (model: Q5000IR). The measurements were taken in nitrogen flow and using a scan rate of 20 °C min⁻¹ in a temperature range from room temperature to 900 °C. Data processing was carried out using the instrument software (TA Universal Analysis). The TG analyses on raw materials and geopolymers were performed in duplicate, and for each sample, the deviation between the two measurements was small, both in terms of the maximum peak temperature in the DTG curves (<5 °C) and the mass loss percent of each step (usually <0.5%). Calcined raw materials underwent single TG measurement.

Differential scanning calorimetry (DSC): DSC measurements were taken using a TA Instruments DSC Discovery 250 operating under a nitrogen flux of 50 mL min⁻¹, with a scan rate of 10 °C·min⁻¹, in the temperature range of -40–300 °C. Data processing was carried out using the instrument software (TRIOS). The peak area, calculated by defining a linear baseline on the desired temperature range, was normalized for the mass loss measured by TGA curves over the same temperature range, to obtain an average molar heat of dehydration.

Accelerated aging methodologies and related experimental setups: Representative samples were subjected to accelerated aging by exposure to ultraviolet (UV) light or acetic acid vapor. For the UV exposure, a medium-pressure mercury lamp (Polymer 400 W, Helios Quartz) was used. The irradiance at 15.0 cm was 13.4 W cm⁻² at 254 nm and 18.4 W cm⁻² at 365 nm. The samples that were pulverized (with a mortar) were exposed for 5 hours under the lamp. For exposure to acetic acid vapors, approximately 20 mL of

glacial acetic acid was placed in the bottom of a borosilicate glass desiccator to ensure an atmosphere saturated with its vapors. The samples were stored in the desiccator for 96 h, keeping the temperature constant at 25 °C for all the exposure time. The aged samples were then analyzed by TGA (the powder), in order to observe possible changes in the thermal stability induced by the accelerated aging conditions.

Statistical analysis of the data by principal component analysis (PCA)

Statistical processing of the data obtained by TGA was performed by PCA. In particular, the mass losses in the following temperature intervals were used as input in the PCA: (1) 30–200 °C; (2) 400–600 °C; (3) 600–900 °C; and (4) % residue at 900 °C. PCA was performed based on the correlation matrix to rescale the relative mass of the residue whose value is significantly larger than the other variables, in accordance with what was done in previous work [20]. A second PCA was performed including mineralogical composition and thermal data of the geopolymer samples alone. Also, in this case, the PCA was performed based on the correlation matrix. The statistical data treatment was carried out using XLSTAT software by Adinsoft.

Results and discussion

Raw materials

The raw materials (as-is and calcined) were analyzed by TGA, DSC, and XRD. The curves of representative samples (NU and PP) are reported in Fig. 2, while the complete set of results is reported in Table S2-3.

The curves of the raw materials showed three or four different steps of mass loss, with small differences related to different origin of clays. Each loss was caused by different thermal events, identified in analogy with the literature [20, 21]: (1) the first in a temperature range of 40–150 °C (3–5% mass loss), attributed to surface, hygroscopic, or zeolitic water loss; (2) the second in a range of 200–400 °C (<0.6%), attributed to structural water removal by aluminosilicate; (3) the third with a maximum of the DTG curve around 500 °C (2.3–5.3%) related to dehydroxylation of silicates; and (4) the fourth with a maximum of the DTG curve around 700 °C. This last signal was mainly related to decarbonation phenomena and showed the greater variability in the mass loss percent among different samples according to their origin, ranging from a minimum of 1% to a maximum of 7% for the Plio-Pleistocenic clays, while the Numidian clays showed no significant losses around this temperature. The calcined samples showed, as expected, a pattern of

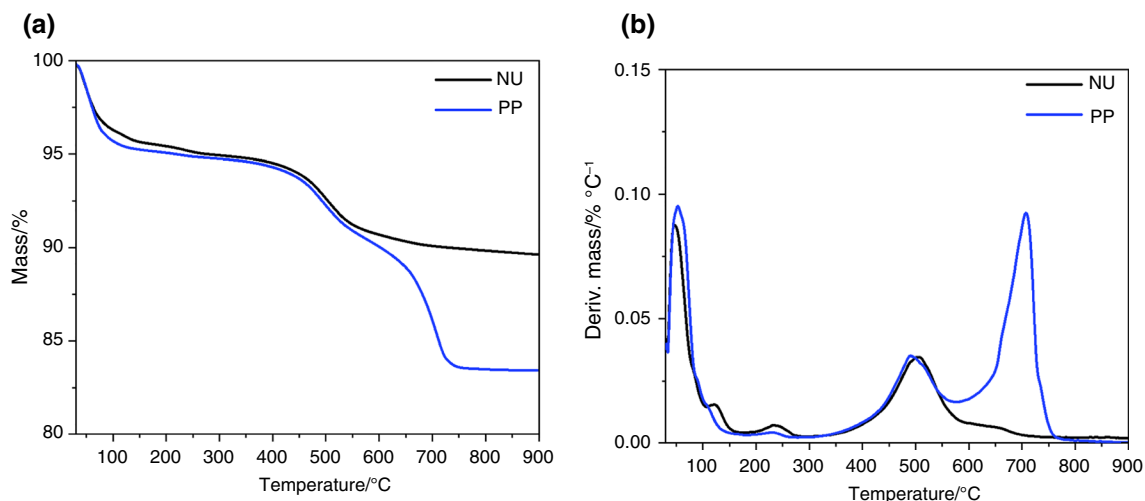


Fig. 2 Representative **a** TG and **b** DTG profiles of PP and NU, recorded at $20\text{ }^{\circ}\text{C min}^{-1}$ in N_2

much smaller mass losses. In fact, they displayed a mass loss below $150\text{ }^{\circ}\text{C}$, lower than 1.7%, and two mass losses at around $400\text{ }^{\circ}\text{C}$ and $645\text{ }^{\circ}\text{C}$, respectively, even smaller in magnitude, thus resulting in a residual value at $900\text{ }^{\circ}\text{C}$ at least 5% higher than the respective non-calcined samples.

DSC measurements (Table S3) provided additional insights into the samples' dehydration processes. All the curves showed an endothermic loss associated to the sample dehydration. Two maxima could be distinguished in samples RP and NU (at around $60\text{--}70\text{ }^{\circ}\text{C}$ and $140\text{ }^{\circ}\text{C}$, respectively), confirming that dehydration process occurs according to different steps. Differently, the second dehydration process was less pronounced in the samples MU and PP, which present the first maximum at the same temperature of RP and NU, followed by a shoulder at higher temperatures. The integral heat associated to water removal in the interval from ambient temperature to about $250\text{ }^{\circ}\text{C}$, evaluated from the area subtended to the DSC curves, was normalized for the mass loss measured by TGA over the same temperature range, to obtain an average molar heat of dehydration. The values of ΔH obtained (Table S3) ranged from a minimum of 43.7 kJ mol^{-1} to a maximum of 49.7 kJ mol^{-1} . These values, compared to the evaporation heat of pure water (which ranges from 44.0 kJ mol^{-1} [28] at $25\text{ }^{\circ}\text{C}$ to 31.8 kJ mol^{-1} at $250\text{ }^{\circ}\text{C}$) confirmed that water present is not simply adsorbed onto the surface of the material but is also at least partially bound.

X-ray diffraction results of all clay raw materials were characterized by clay minerals quartz and feldspars in order of abundance (Fig. 3). However, differences in calcite content allowed us to distinguish PP, MU, and RP samples, in which calcite is present, from NU and VC where it is absent. Thermal treatment at $700\text{ }^{\circ}\text{C}$ for 3 h caused the disappearance of kaolinite XRD signals, while smectite peaks were

strongly reduced. Furthermore, in the carbonate-bearing samples, calcite peaks were strongly reduced.

Geopolymers

Raw materials were used to build geopolymers following the procedures described in the Experimental Section. Among all the raw materials analyzed, only PP and NU samples were used, due to their chemical and mineralogical composition. The list of all the samples prepared is reported in Table S1. The geopolymers were subjected to TG, DSC, and XRD analyses to assess their thermal stability and mineralogical composition. The results of thermal analyses for the different samples are reported in Table S3-4. Representative TGA profiles are shown in Fig. 4.

Thermal behavior of Plio-Pleistocenic clay-based geopolymers

The samples PP700-4M, PP700-6M, and PP700-8M were obtained using NaOH solutions of different molarities on a Plio-Pleistocenic clay calcined at $700\text{ }^{\circ}\text{C}$. The geopolymer samples showed an increase in water losses below $160\text{ }^{\circ}\text{C}$ with increasing NaOH concentration (from 6.8%, to 9.6%, to 13.4%). Above $200\text{ }^{\circ}\text{C}$, the degradation pattern of geopolymer samples was increasingly less defined with respect to that of the calcined raw material, possibly indicating progressively more cross-linked samples. Moreover, a general increase in the mass losses (4 to 7%) in the range of $400\text{--}650\text{ }^{\circ}\text{C}$, mainly dominated by dehydroxylation phenomena, was observed. The mass loss occurring around $700\text{ }^{\circ}\text{C}$, related to decarbonation, decreased with respect to the raw material but is in line with the mass loss of calcined material. The overall effect was a

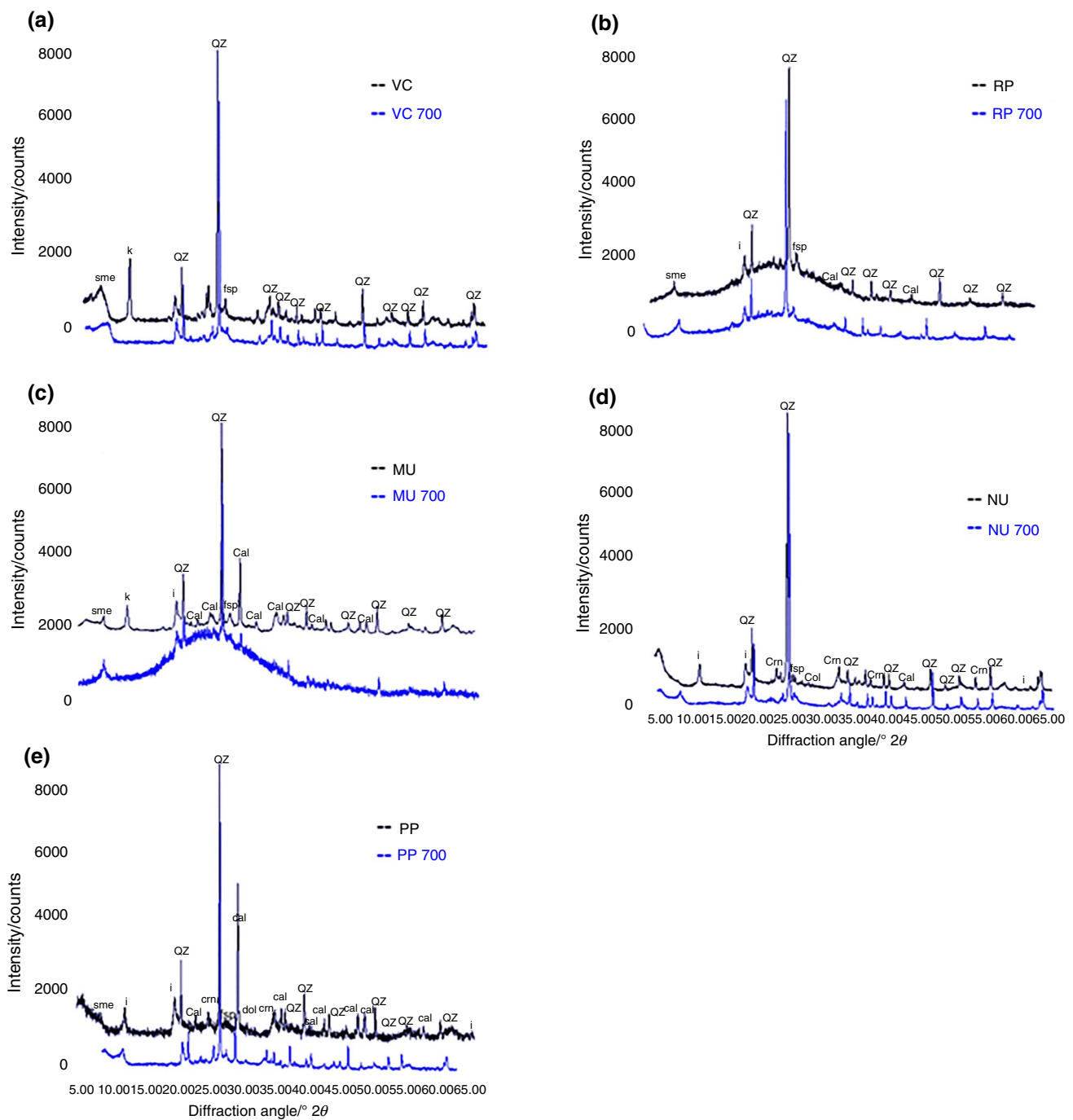


Fig. 3 XRD patterns of Sicilian clayey raw materials and the same calcined at 700°C for 3h: **a** VC: Variegated clay; **b** RP: Marly clay sampled near Roccapalumba; **c** MU: Marly clay sampled near Vicari; **d** NU: Numidian clay; and **e** PP: Plio-Pleistocenic clay. In black dif-

fractometric patterns of clay raw materials and in blue those of calcined clay. *Qz* Quartz; *I* Illite; *Sme* Smectites; *Fsp* Feldspars; *Crn* Corundum; *Dol* Dolomite; *Cal* Calcite; *K* Kaolinite

consequent reduction of the residue at 900 °C from 84.9%, to 79.9%, to 79.3% observed when increasing the NaOH molarity. Further addition of sodium silicate R3 (i.e., SiO₂/Na₂O mass ratio of 3) in the PP700S-4M, PP700S-6M, and

PP700S-8M samples did not substantially change the mass loss profiles.

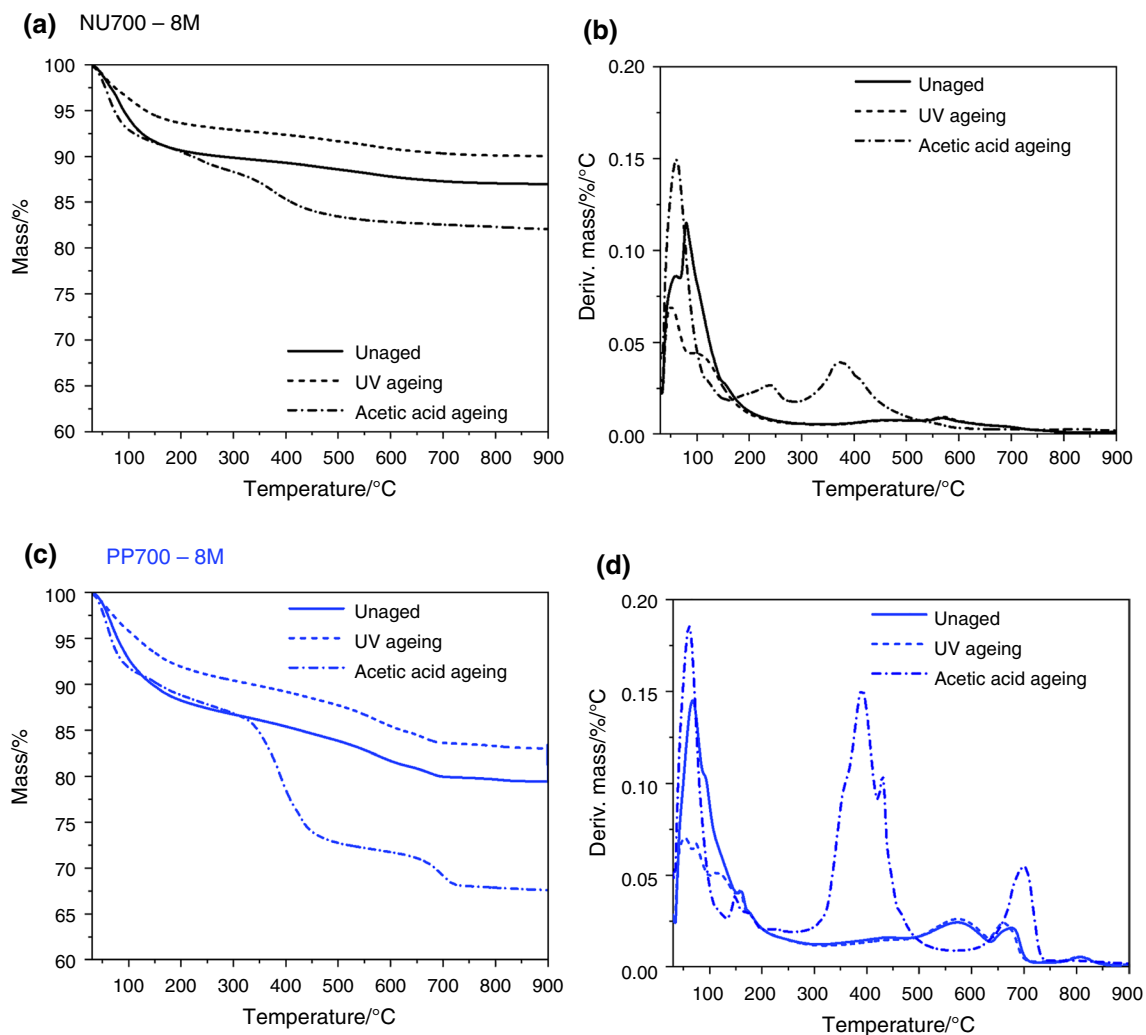


Fig. 4 Representative TG and DTG profiles of the geopolymers: NU700-8M (a and b) and PP700-8M (c and d) unaged (full lines) or subjected to artificial aging by UV irradiation (dashed line) or exposure to acid acetic vapors (dashed-dotted lines)

Thermal behavior of Numidic clay geopolymers

The NU700-4M, NU700-6M, and NU700-8M geopolymers showed in the DTG curve a much more structured and intense signal pattern than that of the respective raw materials, ascribable to the elimination of both surface and weakly bound water and confirming the entrapment of water during the geopolymerization process. The subsequent mass loss (associated to dehydroxylation) globally shifted to higher temperatures with increasing the NaOH concentration: The DTG curve of NU700-4M showed a relative maximum around 460 °C (1.6% of loss), NU700-6M showed a relative maximum around 444 °C (1.8% of loss), while in NU700-8M, the maximum was shifted up to 567 °C, and the signal around 466 °C appeared as a shoulder, indicating a higher polymerization degree for the latter. An additional small loss (0.2–0.5 %) appeared

in both samples NU700-6M and NU700-8M, probably associated to the removal of atmospheric CO₂ absorbed by the alkali matrix. The addition of silicate R3 (samples: NU700S-4M, NU700S-6M, and NU700S-8M) led to a general simplification of the mass loss curves. In this case, the signal attributable to decarbonation was absent or barely noticeable. The most relevant differences observed in the NU700S series concerned the pattern of water loss at low temperatures (below 150 °C). The first two significant peaks in the DTG profile, with a relative maximum at around 50 °C and 70 °C, respectively, remained at approximately the same temperature in all the samples, but they varied in relative intensity. The third contribution, visible as a shoulder on the DTG curve, gradually shifted to higher temperatures (from 99 °C for NU700S-4M to 108 for NU700S-6M to 120 °C for NU700S-8M). This increase in temperature may indicate a strengthening of the bonds, but it could also indicate a

situation of greater confinement of water deriving from a higher degree of cross-linking.

Artificial aging

As the final aim of the geopolymers preparation is their use in buildings restoration, they were subjected to artificial aging conditions, to test their resistance to atmospheric agents, e.g., solar radiations or acid vapors. Thermogravimetric analyses on geopolymer samples exposed to UV irradiation and acetic acid vapors (see Table S5 and Fig. 4) were performed in order to investigate this topic. The UV exposure on the analyzed samples did not appear to markedly alter the thermal loss profile of the different geopolymers. The only significant change is a decrease in mass loss in the temperature range below 250 °C, where the elimination of surface and weakly bound water occurs, with a consequent redistribution of other percentage losses. Given the configuration of the experimental setup, it is likely that the water loss of the samples during UV exposure is a result of the thermal radiation from the lamp and the laminar air flow under the hood. On the other hand, exposure to acetic acid vapors had significant effects on the mass loss curves of most of the samples studied. In fact, the samples generally showed higher losses than the unexposed ones, and the residue at 900 °C is always lower. Particularly significant were the mass losses in the temperature range of 250–700 °C, in which structural water elimination and dehydroxylation occur. The observed losses were higher than that of corresponding unexposed samples, and the related DTG peaks and shoulders shift toward lower temperatures. Even below 250 °C, the exposed samples showed a higher mass loss, although this effect can be partly due to the residual acetic acid (boiling point: 118 °C [29]) adsorbed on the surface of geopolymer during exposure. The combined effect of lower degradation temperatures, higher mass losses, and lower residual at 900 °C suggested an overall lower thermal stability of the treated samples: Acetic acid may likely induce partial depolymerization. The only sample found to be inert to the action of acetic acid vapors was the geopolymer based on 8M NaOH-activated Numidian clay with silicates added (i.e., sample NU700S-8M), which showed a completely superimposable loss profile compared to the unexposed sample.

XRD of geopolymer samples

In this paper, we used the XRD results of geopolymeric binders reported in [25]. The mineralogical phases detected in the thermally treated raw material were still present in all the geopolymers synthesized. Furthermore, in samples activated with NaOH 6M and 8M, new crystalline phases such as zeolites (Na-faujasite and/or garronite) and, in

sample PP700-6M, hydrated carbonate (pirssonite) appear. Finally, the diffractometric patterns showed a large band in the 20°–40° 2θ range due to the presence of amorphous polycondensed gel.

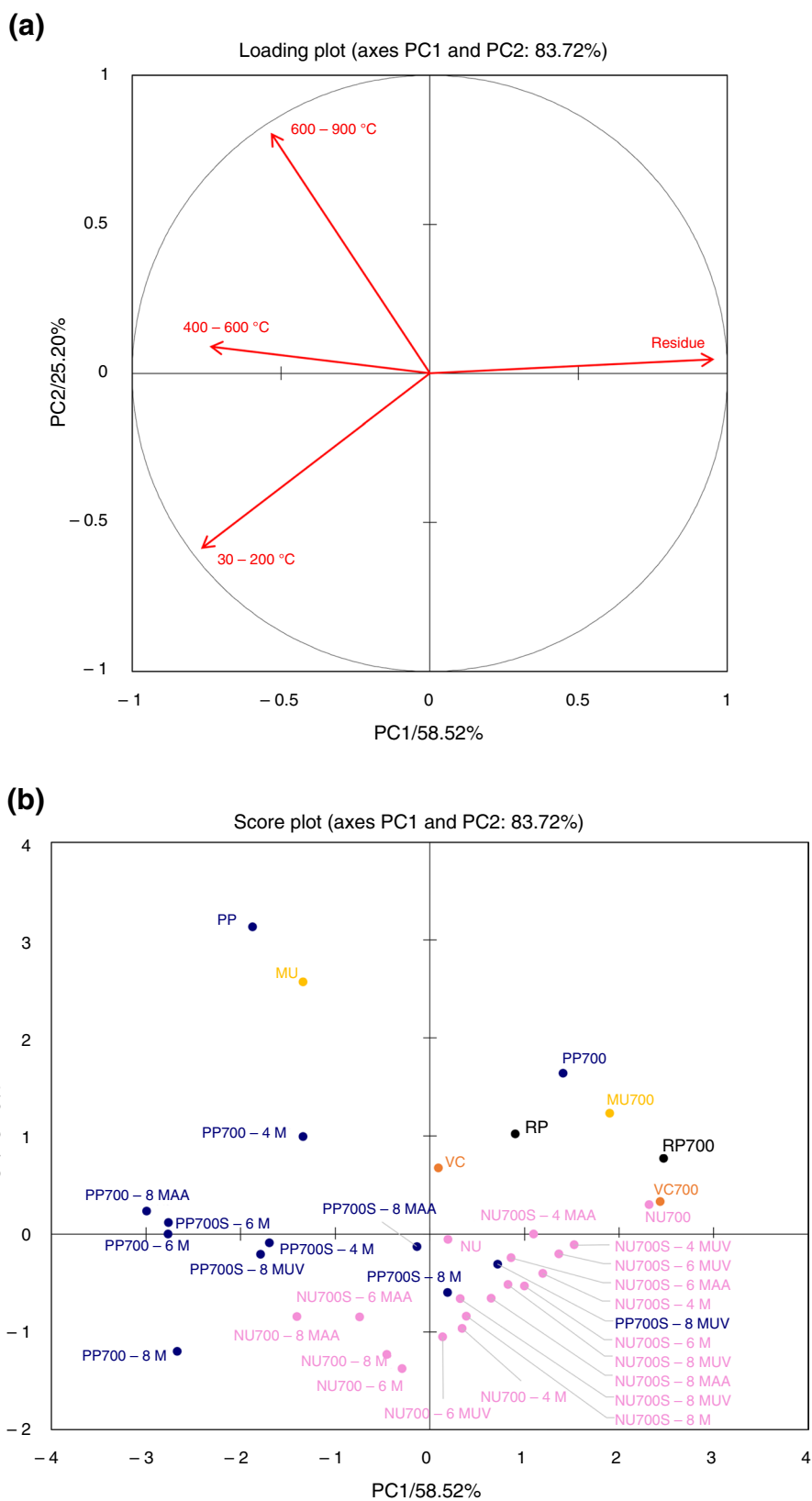
Statistical analysis by principal component analysis

From the thermogravimetric data reported in Tables S2, S4, and S5, we extracted a set of meaningful parameters (i.e., % mass losses in the temperature ranges 30–200 °C, 400–600 °C, and 600–900 °C and % residue at 900 °C) on which we performed multivariate statistical analysis. The statistical analysis by PCA allowed to better identify the differences observed in the thermal behavior studied for the different samples. It also highlighted possible correlations between the synthesis process of the geopolymers and the presence of different additives on the thermal stability of the materials to be observed. The aforementioned statistical method has been widely used for the classification of archaeological ceramics [30, 31] and in geological applications. Furthermore, as reported in our previous work [21], the use of PCA allowed the identification of subgroups within a large group of raw geomaterials, grouped according to mineralogical composition and thermal degradation. The loading (a) and score plots (b) are reported in Fig. 5.

The results of PCA show that the first component (PC1) accounts for 58.52% of the variance explained, while the second component accounts for 25.20%. Moreover, by observing the loading plot (Fig. 5a), the variables that contribute most to sample separation are the mass losses in the 30–200 °C and 400–600 °C ranges and the residue. The geopolymer samples mostly lie in the third and the fourth quadrants. In particular, the NU-based geopolymer samples appear distributed along a straight line with a positive slope passing below the axes' origin, while PP-based geopolymers show no definite trend and are scattered mainly in the third quadrant. In the first quadrant (i.e., with positive values of PC1 and PC2) lie all the raw materials calcined at 700 °C and two non-calcined raw materials (VC and RP), while NU is located at just negative values of PC2, very close to the origin of the axes. The remaining two raw materials, PP and MU (which show significant losses in the 600–900 °C range), lie somewhat isolated in the second quadrant. NU-based samples are clustered according to the presence or the absence of R3 silicate.

For PP-based samples, increasing the concentration of the NaOH solution used for activation generally shifts the samples toward more negative PC2 values, while the effect on PC1 is less unique. In fact, the increase in NaOH concentration causes higher mass losses in the 30–200 °C range and, conversely, lower residue values. The same behavior was observed for the NU-based samples added with silicates.

Fig. 5 Loading plot **a** and score plot **b** obtained from PCA on thermogravimetric data using correlation matrix



The samples artificially aged by UV irradiation (namely PP700-8MUV, PP700S-8MUV, NU700-6MUV, NU700-8MUV, NU700S-4MUV, NU700S-6MUV, and NU700S-8MUV) tend to have higher positive values of PC1 and PC2 compared to the unaged samples, as they have higher residue values and lower mass loss values in the 30–200 °C range. As observed above, this could be due to the dehydration phenomena induced by the thermal effect of irradiation. Exposure to acetic acid vapors generally causes a higher mass loss in the 30–200 °C and 600–900 °C temperature ranges and a decrease in the residue values. In fact, the samples PP700-8MAA, NU700-8MAA, and NU700-6MAA are located at negative values of PC1 as they showed a significant mass loss in the 30–200 °C and 400–600 °C ranges, while the other aged samples, namely all the NU700S samples, are located at positive values of PC1 as they showed higher residue values. However, no significant difference was observed in the score plot position of the samples aged by acetic acid exposure and the corresponding non-aged samples, probably due to compensation effects.

In order to determine a possible correlation between the mineralogical composition and the thermal degradation of the geopolymer samples alone, a PCA was carried out including the thermogravimetric data and the mineralogical data obtained from the XRD analysis. In this case, only the mineralogical components that allowed the samples to be distinguished were taken into account (thus excluding the content of the minerals quartz, feldspar, illite, and corundum, which were equally present in all samples). In terms of composition, X-ray analysis provides only summary indications of the relative abundance of the different mineralogical forms, classified as absent, scarce, moderate, and abundant. Given the requirement to parameterize this classification to perform the PCA, it was evaluated to assign a value of zero for an absent mineralogical form and 1, 2, or 3 to indicate an increasing amount. In this case, given the different nature of the data treated by multivariate analysis, the PCA was performed using the correlation matrix. This procedure corresponds to autoscaling the data and allows the comparison of data relating to completely different variables. The biplot obtained is reported in Fig. 6.

By observing the biplot, it is worth noting that there is a correlation between thermal degradation and chemical composition of the geopolymer samples. In fact, some mineralogical composition-related variables overlap with thermal degradation-related variables. In particular, a positive correlation is observed between the mass loss in the 30–200 °C temperature range and the amount of pirssonite (Pss) and garronite (Grn), whereas a negative correlation is observed between these variables and the residue. Moreover, the mass loss in the 600–900 °C temperature range is positively correlated with the amount of smectite (Sme) and calcite (Cal), whereas a negative

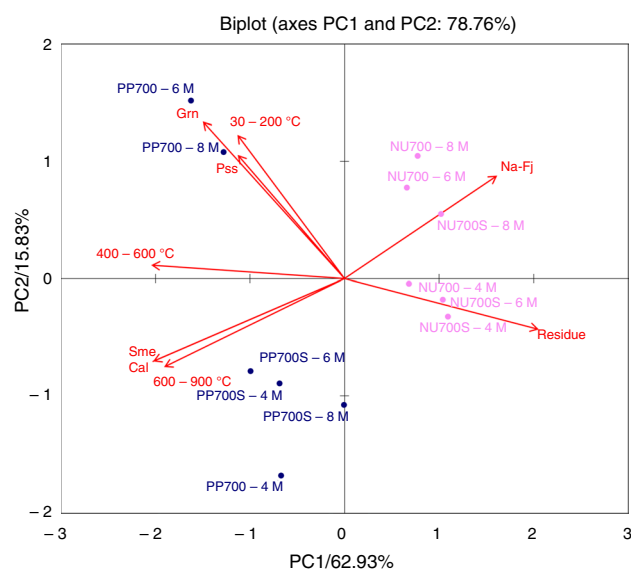


Fig. 6 Biplot obtained from PCA on thermogravimetric and mineralogical data using a correlation matrix

correlation is observed with the amount of faujasite (Na-Fj). However, it should be noted that the variables related to Sme and Cal amount are exactly overlapped, since these minerals are present in the same sample subset (PP-based geopolymers) and in the same amount, thus not allowing any discrimination between them. Therefore, samples containing Sme and Cal showed a higher mass loss in the 600–900 °C temperature range, although it is probable that this correlation is mainly due to the presence of calcite (CaCO_3), which is known to exhibit decarbonation phenomena around 700 °C, as already described (par. "Geopolymers"). On the contrary, samples containing a higher amount of faujasite (Na-Fj) exhibited a lower mass loss in this temperature range. The samples containing higher amounts of Pss and Grn showed higher mass loss in the 30–200 °C temperature range and lower residue. It would appear that the presence of these mineralogical forms correlates with a higher amount of absorbed or weakly bounded water.

Looking at the distribution of the samples, it can be observed that all the PP-based geopolymer samples are placed at negative PC1 and PC2 values, except for PP700S-4M which has a positive PC1 value, albeit less than 1. On the other hand, all NU-based geopolymer samples show positive PC1 values and both positive and negative PC2 values. This distribution is mainly due to the chemical composition, as only NU-based samples contain Na-Fj, while only PP-based samples contain Sme and Cal. Furthermore, all NU-based samples show higher residue values, while only PP-based samples show a mass loss in the 600–900 °C temperature range. Samples PP700-8M

and PP700-6M are placed at negative PC1 and positive PC2 values as they are the only samples containing Pss and Grn.

Dehydration processes by differential scanning calorimetry

DSC measurements provided additional insights into the dehydration processes, in terms of the binding energy of the different water molecules present (surface adsorbed water, zeolitic water, and water segregated between layers or in structural channels). The overall set of data is reported in Table S3, and curves obtained for representative samples are reported in Fig. 7.

The absence of any endothermic signal (related to water melting), even at $-40\text{ }^{\circ}\text{C}$, is likely due to the water confinement into small micro- and nanocavities [32]. The observed signal (a unique peak with a triangular shape with the maximum at around $90\text{ }^{\circ}\text{C}$ and different shoulders) was related to the evaporation of water variously adsorbed or confined in the sample nanostructure. The different dehydration processes observed cannot be distinguished, as they are partially overlapped [21]. The heat associated to water removal, calculated by the peak area normalized for the mass loss obtained by TGA in the same temperature interval, was in all the cases higher than the evaporation heat of free water (which ranges between 44.0 kJ mol^{-1} at $25\text{ }^{\circ}\text{C}$ [28] and 31.8 kJ mol^{-1} at $250\text{ }^{\circ}\text{C}$), confirming that the water present is not simply adsorbed on the surface but is also involved in interactions with the material, giving a slight increase in the heat required for its elimination. The samples with the higher ΔH are the geopolymers PP700-8M and PP 700S-8M made by Plio-Pleistocenic clays activated with NaOH 8M, with a ΔH of 50.7 and 50.1 kJ mol^{-1} ,

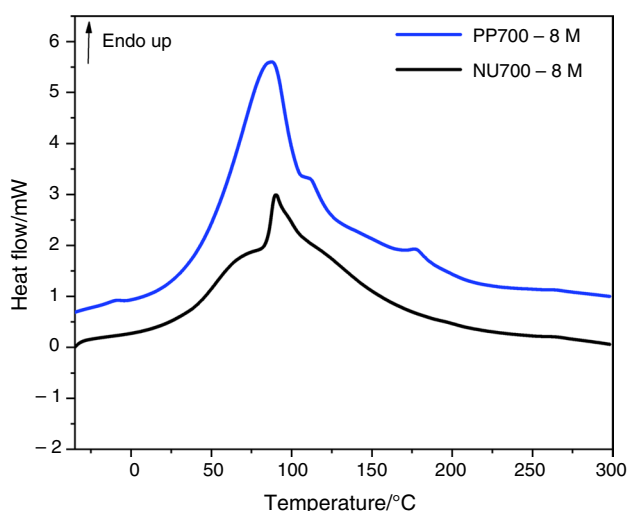


Fig. 7 Differential scanning calorimetry of the geopolymers PP700-8M and NU700-8M, performed at a constant heating rate ($10\text{ }^{\circ}\text{C min}^{-1}$) in the temperature range of $-40/300\text{ }^{\circ}\text{C}$

respectively, in accordance with the behavior observed in TGA experiment, compatible with a higher cross-linking degree and higher amount of water entrapped in the geopolymer matrix.

Conclusions

In this paper, the thermal properties of a novel set of raw materials and geopolymers made from clay sediments with different geological formations were extensively explored.

TGA analyses on raw materials allowed us to study the degradation process of the samples highlighting differences due to the material origin. Additional insights on the dehydration process and the mineralogical composition of the materials were obtained by DSC and XRD, respectively. The same analyses performed on the calcined samples showed a decrease in water adsorbed on the material surface, the disappearance of kaolinite, and the reduction of smectite and calcite (in samples with carbonates).

In a second moment, the calcined Plio-Pleistocenic and Numidian clays were used to prepare a series of geopolymers by alkaline activation with or without the addition of silicate. Thermal degradation of the samples (evaluated by TGA and DSC) showed an increased degree of polymerization in the samples in which a more concentrated NaOH solution was used during their preparation. The thermal degradation of the samples and their mineralogical composition presented a correlation highlighted by a PCA made with a correlation matrix, which allowed the comparison of data related to different variables. In particular, we observed that the presence of the smectite and calcite mineralogical phases is majorly responsible for the mass loss occurring at $600\text{--}900\text{ }^{\circ}\text{C}$, related to decarbonation. Finally, the degradation of samples subjected to artificial aging (by UV irradiation and exposure to acid acetic vapors) was studied, highlighting that the latter may induce partial depolymerization of the samples. The overall data collection will be useful for any future application of these materials.

Supplementary Information The online version contains supplementary material available at <https://doi.org/10.1007/s10973-024-13226-0>.

Author contributions EP and CP were involved in investigation, data curation, methodology, and writing—original draft; MF and AS were involved in investigation, methodology, and writing—original draft; SP contributed to investigation and methodology; RC helped with investigation; LB was involved in conceptualization, data curation, supervision, and writing—review and editing; and MRT, PM, GB, and CD participated in conceptualization, supervision, and writing—review and editing.

Funding Open access funding provided by Università di Pisa within the CRUI-CARE Agreement. This study was funded by the project “Sicilia Eco Tecnologie Innovative–SETI” n. 08CL4120000131 and by University of Pisa (PRA_2022_34).

Data availability Raw data will be made available upon request.

Declarations

Conflict of interest The authors have no relevant financial or non-financial interests to disclose.

Open Access This article is licensed under a Creative Commons Attribution 4.0 International License, which permits use, sharing, adaptation, distribution and reproduction in any medium or format, as long as you give appropriate credit to the original author(s) and the source, provide a link to the Creative Commons licence, and indicate if changes were made. The images or other third party material in this article are included in the article's Creative Commons licence, unless indicated otherwise in a credit line to the material. If material is not included in the article's Creative Commons licence and your intended use is not permitted by statutory regulation or exceeds the permitted use, you will need to obtain permission directly from the copyright holder. To view a copy of this licence, visit <http://creativecommons.org/licenses/by/4.0/>.

References

- de Brito J, Kurda R. The past and future of sustainable concrete: a critical review and new strategies on cement-based materials. *J Clean Prod.* 2021;281:123558.
- Davidovits J. Geopolymers: ceramic-like inorganic polymers. *J Ceram Sci Technol.* 2017;8:335–50.
- van Deventer JSJ, Provis JL, Duxson P, Brice DG. Chemical research and climate change as drivers in the commercial adoption of alkali activated materials. *Waste Biomass Valoriz.* 2010;1:145–55. <https://doi.org/10.1007/s12649-010-9015-9>.
- Provis JL, Bernal SA (2013) Binder chemistry–blended systems and intermediate Ca content. In: Alkali activated materials: State-of-the-art report, RILEM TC 224-AAM pp.125–144. Springer Netherlands
- Xue L, Zhang Z, Wang H. Hydration mechanisms and durability of hybrid alkaline cements (HACs): a review. *Constr Build Mater.* 2021;266:121039.
- Khalifa AZ, Cizer Ö, Pontikes Y, Heath A, Patureau P, Bernal SA, et al. Advances in alkali-activation of clay minerals. *Cem Concr Res.* 2020;132:106050.
- Barone G, Finocchiaro C, Lancellotti I, Leonelli C, Mazzoleni P, Sgarlata C, et al. Potentiality of the use of pyroclastic volcanic residues in the production of alkali activated material. *Waste Biomass Valoriz.* 2020;12(2):1075–94.
- Blanco I, D'Angelo A, Viola V, Vertuccio L, Catauro M. Metakaolin-based geopolymers filled with volcanic fly ashes: FT-IR, thermal characterization, and antibacterial property. *Sci Eng Compos Mater.* 2023;30:20220192. <https://doi.org/10.1515/secm-2022-0192/html>.
- Duxson P, Fernández-Jiménez A, Provis JL, Lukey GC, Palomo A, van Deventer JSJ. Geopolymer technology: the current state of the art. *J Mater Sci.* 2007;42:2917–33. <https://doi.org/10.1007/s10853-006-0637-z>.
- Toniolo N, Boccaccini AR. Fly ash-based geopolymers containing added silicate waste. A review. *Ceram Int.* 2017;43:14545–51.
- Segura IP, Luukkonen T, Yliniemi J, Sreenivasan H, Damø AJ, Jensen LS, et al. Comparison of one-part and two-part alkali-activated metakaolin and blast furnace slag. *J Sustain Metall.* 2022;8:1816–30. <https://doi.org/10.1007/s40831-022-00606-9>.
- Fugazzotto M, Cultrone G, Mazzoleni P, Barone G. Suitability of ceramic industrial waste recycling by alkaline activation for use as construction and restoration materials. *Ceram Int.* 2023;49:9465–78.
- Fugazzotto M, Mazzoleni P, Lancellotti I, Camerini R, Ferrari P, Tiné M, et al. Industrial ceramics: from waste to new resources for eco-sustainable building materials. *Minerals.* 2023;13:815.
- Castillo H, Collado H, Droguett T, Vesely M, Garrido P, Palma S. State of the art of geopolymers: a review. *e-Polymers.* 2022;22:108–24. <https://doi.org/10.1515/epoly-2022-0015/html>.
- Palomo A, Maltseva O, Garcia-Lodeiro I, Fernández-Jiménez A. Portland versus alkaline cement: continuity or clean break: “A key decision for global sustainability.” *Front Chem.* 2021;9:705475. <https://doi.org/10.3389/fchem.2021.705475/full>.
- Geraldes CFM, Lima AM, Delgado-Rodrigues J, Mimoso JM, Pereira SRM. Geopolymers as potential repair material in tiles conservation. *Appl Phys A.* 2016;122:197. <https://doi.org/10.1007/s00339-016-9709-3>.
- Hanzlíček T, Steinerová M, Straka P, Perná I, Siegl P, Švarcová T. Reinforcement of the terracotta sculpture by geopolymer composite. *Mater Des.* 2009;30:3229–34.
- Moutinho S, Costa C, Cerqueira Á, Rocha F, Velosa A. Geopolymers and polymers in the conservation of tile facades. *Constr Build Mater.* 2019;197:175–84.
- Fugazzotto M, Occhipinti R, Caggiani MC, Coccato A, Finocchiaro C, Lanzafame G, et al. Restoration feasibility study by using alkali activated mortars based on Mt. Etna volcanic ash: the case study of Monreale Cathedral. *Mater Lett.* 2023;333:133626.
- Pelosi C, Occhipinti R, Finocchiaro C, Lanzafame G, Pulidori E, Lezzerini M, et al. Thermal and morphological investigations of alkali activated materials based on Sicilian volcanic precursors. *Mater Lett.* 2023;335:133773.
- Pulidori E, Lluveras-Tenorio A, Carosi R, Bernazzani L, Duce C, Pagnotta S, et al. Building geopolymers for CuHe part I: thermal properties of raw materials as precursors for geopolymers. *J Therm Anal Calorim.* 2022;147:5323–35.
- Lancellotti I, Catauro M, Ponzoni C, Bollino F, Leonelli C. Inorganic polymers from alkali activation of metakaolin: effect of setting and curing on structure. *J Solid State Chem.* 2013;200:341–8.
- Kamsu E, Leonelli C, Perera DS, Melo UC, Lemougna PN. Investigation of volcanic ash based geopolymers as potential building materials. *Interceram.* 2009;58:136–40.
- Ferone C, Liguori B, Capasso I, Colangelo F, Cioffi R, Cappelletto E, et al. Thermally treated clay sediments as geopolymer source material. *Appl Clay Sci.* 2015;107:195–204.
- Stroscio A, Barone G, Fernández-Jiménez A, Lancellotti I, Leonelli C, Mazzoleni P. Sicilian clay sediments as precursor for alkali activated materials. *Appl Clay Sci.* 2024;253:107350. <https://doi.org/10.1016/j.clay.2024.107350>.
- Moore D M and Reynolds J (1989) X-ray diffraction and the identification and analysis of clay minerals
- Barbera G, Critelli S, Mazzoleni P. Petrology and geochemistry of cretaceous sedimentary rocks of the Monte Soro unit: constraints on weathering, diagenesis, and provenance. *J Geol.* 2011;119(1):51–68.
- Nathan S, Osborne H, Stimson F, Defoe CG (1939) Measurements of heat capacity and heat of vaporization of water in the range 0°–100°C. *J Res Nat Bur Stand* 23
- Lange NA (1967) Handbook of Chemistry. 10th ed
- Cariati F, Fermo P, Gilardoni S, Galli A, Milazzo M. A new approach for archaeological ceramics analysis using total reflection X-ray fluorescence spectrometry. *Spectrochim Acta Part B At Spectrosc.* 2003;58:177–84.
- Walter J, Chesnaux R, Cloutier V, Gaboury D. The influence of water/rock–water/clay interactions and mixing in the salinization processes of groundwater. *J Hydrol Reg Stud.* 2017;13:168–88.

32. Jähnert S, Vaca Chávez F, Schaumann GE, Schreiber A, Schönhoff M, Findenegg GH. Melting and freezing of water in cylindrical silica nanopores. *Phys Chem Chem Phys*. 2008;10:6039.

Publisher's Note Springer Nature remains neutral with regard to jurisdictional claims in published maps and institutional affiliations.

Authors and Affiliations

Elena Pulidori¹ · Chiara Pelosi¹ · Maura Fugazzotto² · Silvia Pizzimenti¹ · Maria Rita Carosi¹ · Luca Bernazzani¹  · Antonio Stroschio² · Maria Rosaria Tiné¹ · Paolo Mazzoleni² · Germana Barone² · Celia Duce¹

✉ Luca Bernazzani
luca.bernazzani@unipi.it

✉ Antonio Stroschio
antonio.stroschio@phd.unict.it

¹ Department of Chemistry and Industrial Chemistry,
University of Pisa, Via Moruzzi 13, 56124 Pisa, Italy

² Department of Biological, Geological and Environmental
Science, University of Catania, Corso Italia 57,
95127 Catania, Italy